






Research Article

Experimental Investigation and Optimization on Friction Stir Welding of Nylon 6A Using Taguchi and ANOVA with Microstructural Analysis

G. S. V. Seshu Kumar ¹, Anshuman Kumar ¹, S. Rajesh ²,
Rama Bhadri Raju Chekuri ² and Amsalu Gosu Adigo ³

¹Department of Mechanical Engineering, Koneru Lakshmaiah Education Foundation (Deemed to be University), Vaddeswaram, Guntur, Andhra Pradesh, India

²Department of Mechanical Engineering, Sagi Rama Krishnam Raju Engineering College, Bhimavaram, Andhra Pradesh, India

³Department of Chemical Engineering, College of Biological and Chemical Engineering, Addis Ababa Science and Technology University, Addis Ababa, Ethiopia

Correspondence should be addressed to G. S. V. Seshu Kumar; svskgajula@gmail.com and Amsalu Gosu Adigo; amsalu.gosu@aastu.edu.et

Received 31 July 2021; Accepted 2 September 2021; Published 18 September 2021

Academic Editor: Samson Jerold Samuel Chelladurai

Copyright © 2021 G. S. V. Seshu Kumar et al. This is an open access article distributed under the Creative Commons Attribution License, which permits unrestricted use, distribution, and reproduction in any medium, provided the original work is properly cited.

Friction stir welding is an environmentally friendly process of joining due to the nonusage of flux, or any shield gas, and it does not produce any harmful gases when compared to the joining process of fusion. Therefore, this article proposes an experimental investigation and optimization technique for studying the process of FSW on nylon 6A or polycaprolactam polymer composite plates. Specifically, the influence of input operating process parameters such as tool rotational speed (TRS), feed rate, and pitch values on the output response parameters like ultimate tensile strength (UTS) and hardness of welded joints is examined. In addition, L_{27} orthogonal array of Taguchi approach is employed for the optimization of design experiments of FSW parameters. The experimental setup is carried out with various process parameter combinations like 500 rpm, 1000 rpm, and 1500 rpm as TRS, and 30 mm, 40 mm, and 50 mm as feed rate by varying the pitch values as 1 mm, 2 mm, and 3 mm. Further, the analysis of variance (ANOVA) is also employed for finding the significant parameters of input process using the regression analysis equations. Finally, microstructural analysis is used to assess the mixing or dispersing uniformity of composites effectively.

1. Introduction

For improving production efficiency and reducing the costs with lower environmental effect in electronic, automobile, and aerospace devices, the benefits of good corrosion resistance, high specific strength, processing ability, and excellent design freedom have the potential in polymers and polymer matrix composites (PMCs) [1, 2]. The joining technology of welding techniques like adhesive bonding and mechanical fastening is required for the large and complex parts fabrication [3]. At the bonding region, stress concentration appears easily for reducing the joint reliability by manipulating the mechanical fastening that results in the

increasing of lightweight design deterioration. Relatively, adhesive bonding is mature that requires long processing cycle. However, humidity resistance, impact resistance, and fatigue resistance are not enough for reducing joint property. The welding process is the best joining technique that includes different kinds, such as electric resistance welding, linear vibration welding, hot plate welding, FSW, and ultrasonic welding, etc. [3]. Three different processes are included in these welding techniques: (a) a layer of molten material formation to be joined on the surfaces, (b) upsetting forms the bonding, and (c) the stage pressure and molten material cools should be maintained for preventing the forming of voids within the weld zone [4]. Spot welding is

performed mainly by ultrasonic welding but need to spend higher costs on tools and machines and more time is required for preparation. For forming the proper joint at a terribly slow rate, a v -groove requires for extrusion and hot gas welding methods. However, the properties rely on the skill level of operator highly. The flatten face is required for friction welding and the higher costs are included for machine parts. FSW has the potential of overcoming the drawbacks of aforementioned welding techniques due to the fact that it has benefits like high joint quality, severe plastic deformation, low temperature and machine/tool consumable costs, low process time, and no preparation [5]. Figure 1 shows the schematic diagram of FSW. In the rotational tool, a pin and a specially designed shoulder are included during FSW method. At a high rotational velocity, the frictions with the workpieces produce material flow to mix, generate frictional heat to smoothen the materials, and combine the welded materials for welding.

As the polymers include the molecules with various chain lengths and do not include definite melting point instead of melting ranges, FSW is not a solid-state process and its thermoplastic polymers are distinct from metal [6]. Some shorter chains of FSW may reach the melting point while applying FSW/P to polymers, whereas longer chains are in solid state. For thermoplastic polymers, FSW was implemented in 1997 and seldom works report due to the immaturity. Nelson et al. [7] have improved different tools to combine thermoplastic polymers. In 2005, and especially after 2009, the systematical research has started on the FSW of thermoplastic polymers [8]. The joining of PMCs and thermoplastic polymers is realized by FSW. These polymer composites are 20% carbon fiber-reinforced PP composite [9], 30% glasses fiber-reinforced PP composite [10], polyethylene terephthalate (PET) [11], polycaprolactam (nylon 6) [12], polymethyl methacrylate (PMMA) [13], acrylonitrile butadiene styrene (ABS) [14], poly carbonate (PC) [15], poly propylene (PP) [16], and different grades of polyethylene (PE) [17]. Raza et al. used a specific developed tool with a grooved conical pin and a concave shoulder based on high-density polyethylene (HDPE) sheet friction stir welded joints [18]. With and without including the ceramic particulates, the joints were manufactured that included silica, graphite, alumina, and silicon carbide (SiC). In addition, the strain rate impact on the tensile properties of welded joints and base material was also studied. In the applications of high strain rate, the significance could be given to the composite joint of SiC-HDPE providing tool design and optimal parameters for stir welding. Jain et al. [19] discussed that the particles dispersion in metal, polymer matrix, and ceramic composites via conventional routes was very tough due to the poor compatibility properties of particles' clustering or agglomeration. The two-pass friction stir processing is used for dispersing the particles of titanium dioxide on the surface of aluminum matrix uniformly. Huang et al. have studied the FSW of PMCs and thermoplastic polymers, dissimilar metal, and polymer FSW, and multifunctional composites fabrication [20]. Further, the future P -related or FSW scientific research and engineering, thermoplastic polymers, and PMCs with the FSW or P -related scientific research and

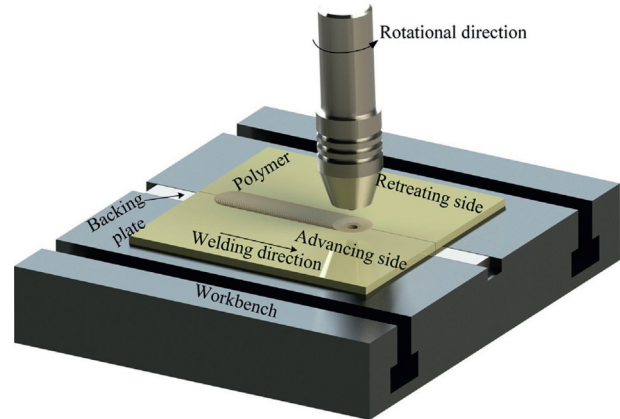


FIGURE 1: Schematic diagram of FSW.

engineering production have also been established. The FSW of nitrile butadiene rubber composite or polyamide 6 with and without an additional heating system was performed in [21]. During the heat assisted FSW, sound joints were obtained based on the heat input and cooling volume regulation. At varying rotational speeds, the tool configuration reliability was analyzed through the mechanical experiments. The creation of defects and improper fusion have been minimized by creating the welds with a heating system that results in substantial development of mechanical properties. They concluded that the maximum tensile strength was 61 MPa with more than 91% of base material mass. Meng et al. [22] have proposed adhesive bonding and multiscale mechanical interlocking for generating the stable hetero junctions between metals and PMCs and improving the mechanical properties. The multiscale mechanical interlocking and adhesive bonding resulted in the overall tensile shear strength of 27 MPa. In [23], authors have studied the Rockwell hardness and impact strength of UHMW polyethylene composites reinforced with nano-hydroxyapatite particles that are FSP-manufactured. Here, the processing metrics were shoulder temperature, strengthening material's volume fraction, tool traverse speed, and spindle speed. It is essential to choose the processing parameters for the variance analysis (ANOVA). The agglomeration of the reinforcing particles and induced voids and channels were caused by the low temperature and higher levels of tool traverse speed and fraction of volume in the microscopic analysis that leads to the reduction of impact strength and the formed composite hardness. The FSW techniques for aluminum alloy sheets for joining different types of thermoplastics with and without fibers are addressed in [24], where an experimental research work is recommended to get insight into the welding parameters' effects on the hybrid joints' efficiency in terms of tensile shear strength. In the instrument geometries investigation, the welding technique and material weldability were considered. For thermoplastic, the FSW is an efficient technique for aluminum joining based on the disclosed findings. Further, microstructural inspection resulted in the strong blending between thermoplastic and aluminum as well as defect-free welds.

The composite sheets of thermoplastic polymer base that include 12% continuous carbon fiber with two advanced speeds of 5/6 and 9 mm/min and two rotational speeds of 355 and 250 rpm in the shape of buttocks were analyzed by Bidgolia et al. [25]. In this low-cost turning system and FSW, a modern tool is used that is made of plain carbon steel st37. In addition, the full relation of materials was shown by the optical microscope images. The development and creation of cavities is contributed by increasing the inlet temperature and they convert into cavities in the tube. Further, the parameters that affect the link efficiency such as the rotational speed and key shoulder diameter were also included. Based on the scanning electron microscopy (SEM), the rotational speed is improved that leads to the continuous carbon fibers grinding and enhanced the tensile strength. Recently, the FSW was applied to glass fiber-reinforced polyamide 6 (PA6) [26]. It is measured in the fiber length distribution and weld strength in the weld seam. The friction stir welded specimen's main effects were investigated based on the tensile strength. According to the higher touch pressures, a tensile strength of 50% of base material strength may be viewed. Additionally, the optical measuring method is implemented and tested for fiber length large-volume measurement. Hajideh et al. used the FSW approach to research the potential of welding of polycarbonate and dissimilar polymethyl methacrylate sheets [27]. The impacts on the process parameters' joints mechanical properties such as heater temperature, rotational, and traverse speeds were analyzed comprehensively. The heater temperatures of 120°C and rotation and traverse speeds of 2100 rpm and 8 mm/min were provided as the optimized mechanical properties of the joint. In the optimal joining state, the welded joint was obtained with a strength equivalent to 98% of polycarbonate and more hardness than the polycarbonate. Authors in [28] have studied the effects on square, threaded, and tapered nylon 6 plates based on three different pin profiles. The method of marker material insert was utilized to analyze the material flow of post-weld specimens visually. The marker material is on the advancing side or retreating side for all pins shown by the uniform vertical stirring with symmetrical pattern. Unlike metals, the pin profile major role was determined in horizontal displacement, where the greatest backward displacement of marker materials was shown by a square pin. Moreover, on any side, the forward flow of all pin profiles was not found. Kumar et al. [29] have studied the feasibility of FSW on the glass-filled nylon 6 composites. Based on an injection molding machine, nylon 6 composites filled with glass were generated and joined with H13 tool steel using a cylindrical pin profile in the FSW process. The factors like tool tilt angle (0°, 1°, and 2°), tool traverse speed (0.2, 0.3, and 0.4 mm/s), and TRS (400, 500, and 600 rpm) with constant standoff distance (0.2 mm) were used in a full factorial experiment design for investigating the morphological and mechanical properties of FSW sections of glass-filled nylon 6 composites. In addition, ANOVA has been employed for estimating the tensile strength significance and percentage elongation process parameters. Practically, the classical metals and unfilled polymers have been replaced using PMCs because of their

superior attributes like low-cost and enhanced toughness with excellent strength/stiffness-to-weight ratio. In addition, for thermoplastic polymers, FSW became one of the important welding methodologies [30].

Thus, this article proposes FSW aspects of PMCs and thermoplastic polymers (new technologies of FSW to eliminate defects, thermomechanical behavior, mechanical properties, and variables of welding process), dissimilar FSW of polymer and metal, and fabrication of multifunctional composites. Therefore, this article proposes an experimental investigation and optimization technique for studying the process of FSW on nylon 6A or polycaprolactam polymer composite plates. Specifically, the influence of input operating process parameters such as TRS, feed rate, and pitch values on the output response parameters like UTS and hardness of welded joints is examined. In addition, L_{27} orthogonal array of Taguchi approach is employed for the optimization of design experiments of FSW parameters. Further, ANOVA is also employed for finding the significant parameters of input process using the regression analysis equations. Finally, microstructural analysis is used to assess the mixing or dispersing uniformity of composites effectively.

2. Materials and Methods

In this work, the nylon 6A is utilized which is a polymer for reproducing the properties of nylon 6,6 with nonviolation of patent on the production. It is relevant to the semicrystalline polyamide. Unlike any other nylons, nylon 6A is not a condensation polymer. But ring-opening polymerization is formed that makes a special case by comparing between addition polymers and condensation. In general, fibers of nylon 6A are tough to deal with because they contain elasticity, high tensile strength, and luster. They are resistant to the chemicals and abrasion highly such as alkalis and acids. Usually, 2.4% of water can be absorbed by the fibers even though it reduces the tensile strength. Moreover, it includes the glass transition temperature of 47°C. Prior to the generation of different color results, nylon 6A can be dyed in a solution path as it is white as a synthetic fiber. The heat protection is up to 150°C, the melting point is at 215°C, the density is 1.14 gm/cc, and the tenacity is between 6 and 8.5 gm/den. 12% of ledeburitic chromium tool steel is included in D3 steel with the great resistance of wears. However, it can be used as cutting tools for shear cutting edges, blanking dies for paper and plastics, sheets up to 4 mm thickness, and rotational shear edges with the thicknesses of sheets up to 2 mm. High chromium 12% tool steel and 2% of high carbon with high wear resistance are the major properties of D3 steel. After making the dies and tools, the hardness is 57 to 58 HRC which is reached using this D3 steel that anneals to easy machining based on its supply condition.

2.1. Tensile Strength Test. For assessing the composites and matrix alloy mechanical behavior, tensile tests are utilized. The matrix alloy and composites were machined to tensile the

specimens with gauge length of 30 mm and a length of 13.5 mm. UTS, often termed as TS, is the maximum stress that a material can withstand while being stretched or pulled before necking, which is when the specimen's cross-section starts to significantly contract. Figure 2 demonstrates the ASTM standard specimen dimensions for UTS.

2.2. Hardness. Practically, the material resistance is measured using shore hardness, where it has several shore hardness scales for determining the hardness of different materials like super soft gels, rigid plates, fibers, rubber, etc. To have the common point of reference for discussing the materials such as super soft gels, rigid plates, fibers, and rubber, the shore hardness scales were discovered to the people. A greater resistance indicates a higher number on the scale to indentation and hence harder materials. Less resistance and thus soft materials are indicated by the lower number of scales.

2.3. Microstructure Analysis. From nylon 6A polymer composite, the samples with metallographic structure were taken that were joined with the method of FSW. In micro and macro size, the structures containing the dynamic recrystallization zone (DCZ), thermomechanically affected zone (TMAZ), heat affected zone (HAZ), and base metal (BM) are investigated. From the welding joints' cross-sectional surfaces, both micro- and macrostructure images have been taken.

2.4. Design of Experiments Using Taguchi Method. This work utilized the Doe method for collecting the data and obtaining the accurate results. Three process parameters like pitch (mm), feed rate (mm/min), and TRS (rpm) were chosen for orthogonal array (L_{27}) and the results are analyzed using MINITAB 19 software. In addition, the HCHCr tool is used to join the work piece and the hardness, and UTS are measured as output responses of FSW joint. Table 1 lists the values of input process parameters with corresponding levels.

2.4.1. Taguchi Method. In the machining processes, the most utilized robust design approach is the Taguchi technique, which was analyzed for finding the controllable parameters with the best characteristics of response in FSW. In the experimental designs, the Taguchi technique is used based on orthogonal array for reducing the uncontrollable components effects while establishing the tests. Owing to the constant distribution of interactions between facts and the input components, Taguchi L_{27} orthogonal array as demonstrated in Table 2 is used for the experiments to minimize the uncontrolled components. The Taguchi design of experiments was evaluated to obtain the data through the conversion it to signal-to-noise (S/N) ratio after completing the trials. In different ways, the standard S/N ratio values are determined and assessed using the intended quality value, with nominal being better, lower being better, and greater being better.

3. Experimental Investigation

This section describes the experimental investigation, which is done to verify the mechanical attributes of FSW on nylon 6A (also known as polycaprolactam material) as shown in Figure 3(a). Here, UTS and hardness are employed as the properties to be investigated before and after the process of FSW. The work is done using an automatic fed vertical milling machine by setting the TRS and feeds accordingly with the taper threaded tool profile consideration as shown in Figure 3(b). Figure 4 illustrates the machining setup of FSW with the following specifications:

- (i) Capacity of motor: 7.5 hp
- (ii) Speed of rotation: 35 to 750 rpm
- (iii) Feed rate: 16 to 800 mm/min
- (iv) Make: HMT
- (v) Length of bed: 1000 × 400 × 450 mm

3.1. The Tool. Tool steel is the mixture of variety of alloy and carbon steels, and they are well-suited for being used as tools due to their suitability, distinctive hardness, ability of holding a cutting edge at elevated temperatures, and resistance to abrasion and deformation. Thus, tool steels can be exploited for shaping of other materials. Tool steels contain six groups such as hot-work, high-speed, shock-resisting, cold-work, water-hardening, and special purpose. Based on the toughness, shock resistance, strength, required surface hardness, working temperature, and cost requirements, the group choice is selected. In this work, HCHCr is considered as tool material and its specifications are given below.

- (i) Tool length: 100 mm
- (ii) Tool tip's diameter: 2 mm
- (iii) The pin length: 4.7 mm
- (iv) Tool shoulder's diameter: 20 mm

3.2. Process. The plates with dimensions are considered as 100 × 50 × 6 mm; then shearing process is used to cut the plates into the required size. Both plates are then clamped to the machine bed as illustrated in Figure 5(a). At the plates joining, a center bit is given the plunge depth and a hole is created to traverse the plates for the tool to be made the FSW, as shown in Figure 5(b). Then, the tool passes on the two plates' intersection after creating the hole when the pressure is applied on the plates using the tool shoulder. Based on the automatic feeds, the tool moves on to the other side of weld. Some time is given for the friction after inserting the tool to develop and the material is heated up to the plates' red-hot condition. However, the time is known as the indentation time and is considered as 5–8 seconds. The plates are considered as the friction stir welded once the tool reaches the other side as demonstrated in Figure 5(c).

4. Results and Discussion

This section describes the results obtained using FSW process of nylon 6A material and HCHCr tool with taper

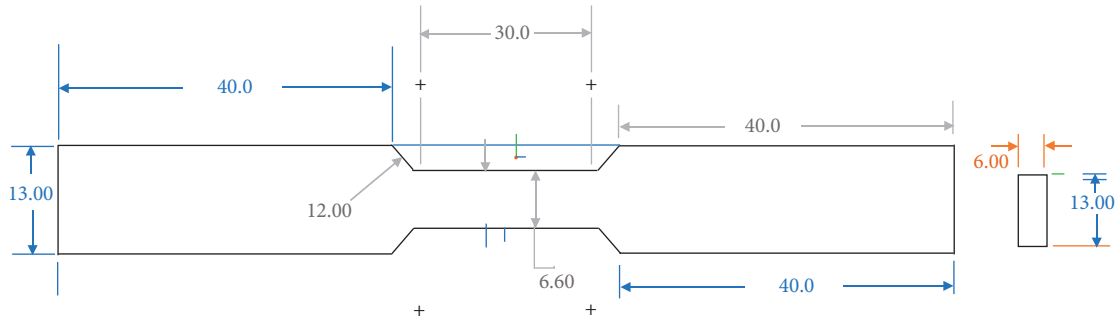


FIGURE 2: ASTM standard specimen dimensions for UTS.

TABLE 1: Input process parameters.

Process parameters	Level 1	Level 2	Level 3
TRS (rpm)	500	1000	1500
Feed rate (mm/min)	30	40	50
Pitch (mm)	1	2	3

threaded tool profile by varying the pitch values. Here, TRS (rpm), feed rate (mm/min), and pitch (mm) are considered as input process parameters while the UTS and hardness are assumed as output parameters, which means the strength of welding is assessed using these UTS, and hardness values. As we need the maximum tensile strength, the input parameters performed the concept of the larger, the better criteria. Table 3 lists the obtained experimental output parameters such as UTS and hardness with the variation in input process parameters like TRS (rpm), feed rate (mm/min), and pitch (mm).

4.1. *Analysis of Variance (ANOVA)*. The ANOVA is employed to measure how the input operating process parameters influence the output response parameters, i.e., mechanical attributes of welded joints, via the association between these two input and output variables, where the

Fisher test is applied to measure the significance degree in these relationships. In this work, the maximum tensile yield stress is analyzed. For each control factor, ANOVA is required to be estimated for accessing the factors impact on response. To investigate which design parameters affect the characteristic significantly, the experimental results are assessed using the method of ANOVA, which can identify the input parameters contributions on UTS and hardness. To detect the process parameters whose variance in the design space impacts the output response metrics, ANOVA is applied while choosing 90% of confidence interval for experimental investigation. If the computed probability (P) value is about 10% or less, the factor significance is considered. After ANOVA, the obtained value of P is demonstrated in Table 4 as well as their significance on output response metrics like UTS and hardness, respectively.

4.2. *Regression Analysis*. After the process of weld joining, the regression analysis is conducted based on the obtained data results. The linear equations are derived that are relevant to the dependent and independent variables, which is performed using MINITAB software and the regression equations are mentioned as follows:

$$\begin{aligned}
 \text{UTS} &= 123.0 - 0.0225A - 3.90B - 20.2C + 0.000004A^2 \\
 &\quad + 0.0449B^2 + 5.6C^2 + 0.000134AB + 0.0056AC + 0.243BC - 0.00197AC^2 - 0.064BC^2, \\
 \text{HARDNESS} &= 115.2 + 0.0372A - 2.382B - 18.5C - 0.000016A^2 \\
 &\quad + 0.03313B^2 + 4.16C^2 - 0.000080AB + 0.01079AC + 0.010BC - 0.00203AC^2 - 0.008BC^2.
 \end{aligned}
 \tag{1}$$

Based on the listed values of R^2 , $\text{Adj-}R^2$, and $\text{Pred-}R^2$ in Table 5, the potency of equation (1) can be realized for predicting the variance inside the design space. After employing ANOVA, the derived model equations were used to estimate the variability within the design space for all output responses based on the results analyzation.

For detecting the control factors, robustness is measured in Taguchi designs that decrease the product or process variability while minimizing the uncontrollable factors' effects (noise factors). Design parameters are control factors

and controllable parameters are process parameters. During product use or production, noise factors cannot be controlled, but they can be controlled during experimentation. For force variability to occur, the noise factors are calculated in a Taguchi designed method. The settings of optimal control factor are detected to make the process or product resistant or robust towards variation against noise factors. The control factor settings are indicated by higher values of S/N ratio that reduce the noise factors impact. The measurement of how the response is varied regarding the target

TABLE 2: Taguchi L_{27} orthogonal array.

S. No.	TRS (rpm)	Feed rate (mm/min)	Pitch (mm)
1	500	30	1
2	500	30	2
3	500	30	3
4	500	40	1
5	500	40	2
6	500	40	3
7	500	50	1
8	500	50	2
9	500	50	3
10	1000	30	1
11	1000	30	2
12	1000	30	3
13	1000	40	1
14	1000	40	2
15	1000	40	3
16	1000	50	1
17	1000	50	2
18	1000	50	3
19	1500	30	1
20	1500	30	2
21	1500	30	3
22	1500	40	1
23	1500	40	2
24	1500	40	3
25	1500	50	1
26	1500	50	2
27	1500	50	3

or nominal value under various noise conditions is measured using the S/N ratio. Based on the experimental objective, different S/N ratios are chosen, and three quality characteristics are introduced by Taguchi, such as larger is better, nominal is better, and smaller is better.

4.3. Process Parameters Effect on UTS. Table 6 lists the response values for S/N ratios of UTS. Figure 6 depicts the input operating process parameters such as TRS, feed rate, and pitch for S/N ratio on UTS, where the deviation of response line is with respect to the horizontal line, which demonstrates that these operating process parameters highly impact the performance measure, which also led to significant influence on UTS. The speed and pitch are the most significant input operating process parameters of machining for UTS in FSW of nylon 6A material with HCHCr tool while the feed rate is the least significant input operating process parameter.

4.4. Process Parameters Effect on Hardness. Table 7 demonstrates the response for S/N ratios of hardness. Figure 7 depicts the input operating process parameters such as TRS, feed rate, and pitch for S/N ratio on hardness, where the deviation of response line is with respect to the horizontal line, which demonstrates that these operating process parameters highly impact the performance measure, which also led to significant influence on hardness. The TRS, pitch,

and feed rate are the most significant input operating process parameters of machining for UTS in FSW of nylon 6A material with the HCHCr tool.

4.5. Microstructure Analysis. From the polymer composite of nylon 6A, the samples with metallographic structure are considered, which are later integrated with the FSW and then examined in detail. FSW joints include the structures that contain thermomechanically affected zone (TMAZ), base metal (BM), heat affected zone (HAZ), and nugget zone as demonstrated in Figure 8. These structures are studied in both micro and macro size. In addition, from the welding joints' cross-sectional surfaces, micro- and macrostructure-based images are taken, which are illustrated in Figure 9.

Based on the TRS and feed rate, structures have been changed. The wide gaps were observed in the joining zones if the welded sample's microstructure was examined with the TRS of 1500 rpm and a feed rate up to 50 mm/min. The less porosity has occurred at the joining zones if the welded sample's microstructure was tested with the TRS of 500 rpm and a feed rate of 30 mm/min. Then, the material is extruded to join better. In the welding center, the gaps and the zones at the bottom of nugget zone are observed. In the welded joints, the amounts of gaps and size increase by increasing the value of feed rate and TRS. In the defects' size, the increment is predicted with the reducing of temperature in the unit time and area.

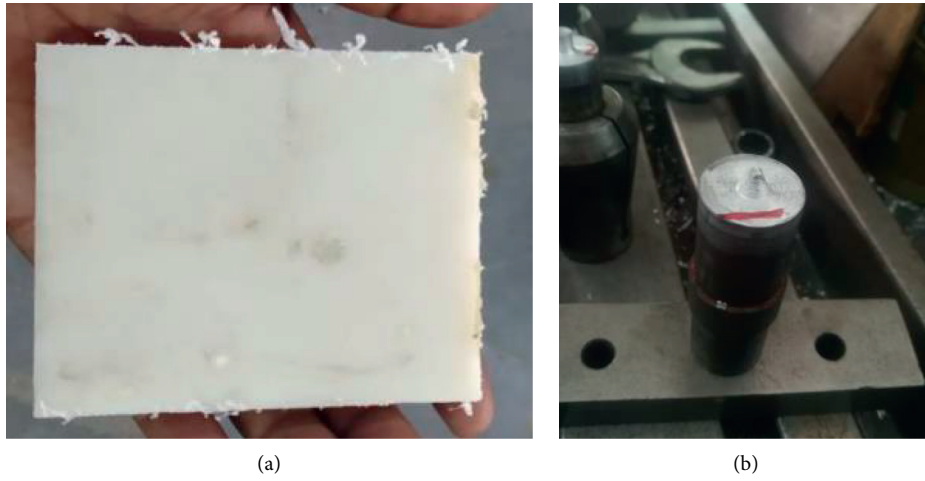


FIGURE 3: (a) Raw material of nylon. (b) Taper threaded tool.



FIGURE 4: Machine used for FSW.

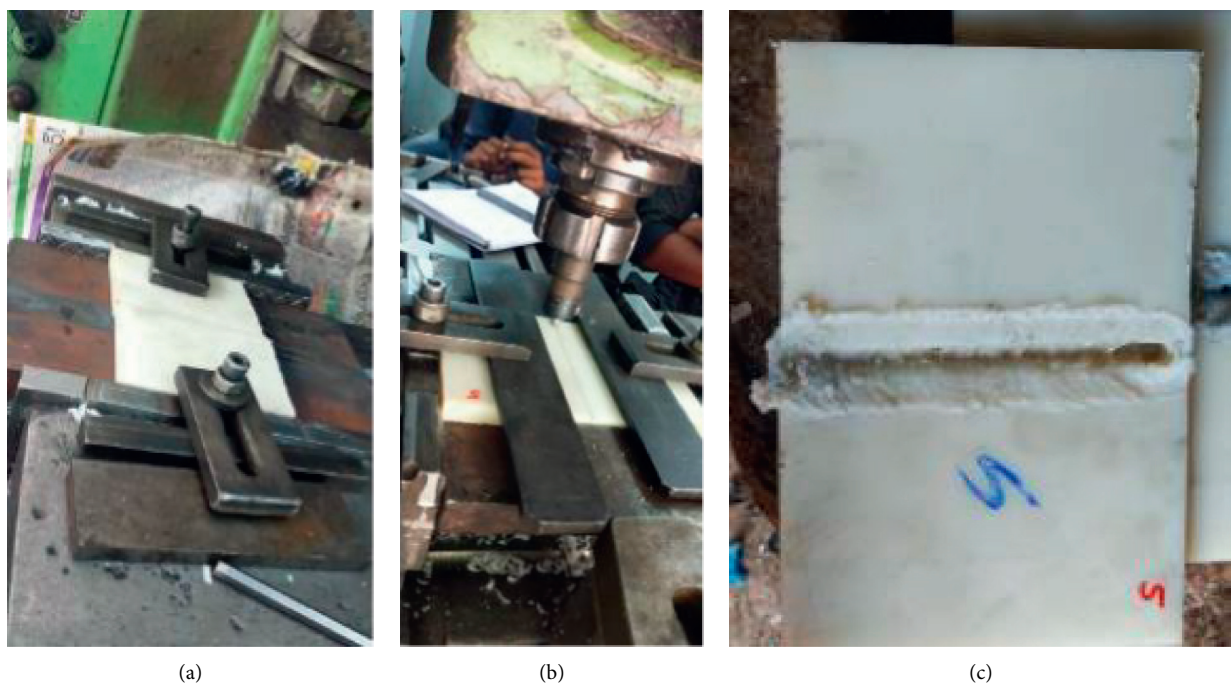


FIGURE 5: (a) Workpiece clamping. (b) FSW process. (c) Final specimen joint.

TABLE 3: Obtained experimental results of UTS and hardness.

S. No.	TRS (rpm)	Feed rate (mm/min)	Pitch (mm)	UTS (N/mm ²)	Hardness
1	500	30	1	32.97	76.00
2	500	30	2	31.34	72.11
3	500	30	3	35.86	73.11
4	500	40	1	17.96	79.33
5	500	40	2	18.95	72.21
6	500	40	3	21.91	75.11
7	500	50	1	32.11	81.33
8	500	50	2	33.32	77.11
9	500	50	3	34.98	78.12
10	1000	30	1	27.92	86.11
11	1000	30	2	21.35	87.12
12	1000	30	3	24.81	88.91
13	1000	40	1	26.52	86.12
14	1000	40	2	23.12	84.13
15	1000	40	3	22.16	85.67
16	1000	50	1	26.17	88.12
17	1000	50	2	22.35	88.90
18	1000	50	3	20.89	89.93
19	1500	30	1	19.34	89.16
20	1500	30	2	20.21	90.45
21	1500	30	3	18.34	92.89
22	1500	40	1	21.78	87.56
23	1500	40	2	22.17	84.13
24	1500	40	3	19.07	87.13
25	1500	50	1	22.67	93.21
26	1500	50	2	21.07	94.22
27	1500	50	3	22.45	95.61

TABLE 4: Major factors and corresponding P values for the process of FSW.

Model	P value	
Factors	UTS	Hardness
A	0.023	0.001
B	0.076	0.004
C	0.040	0.007
A ²	0.060	0.036
B ²	0.045	0.001
C ²	0.030	0.001
AB	0.098	0.080
AC	0.021	0.004
BC	Insign	0.017
AC ²	Insign	Insign
BC ²	0.075	Insign

TABLE 5: Residuals for all the performance measures.

	UTS	Hardness
R^2	0.9024	0.9554
Adj- R^2	0.8992	0.9115
Pred R^2	0.8324	0.8408

TABLE 6: Response for S/N ratios of UTS.

Level	TRS	Feed rate	Pitch
1	28.92	27.99	27.88
2	27.53	26.60	27.36
3	26.33	28.20	27.54
Delta	2.59	1.60	0.52
Rank	1	2	3

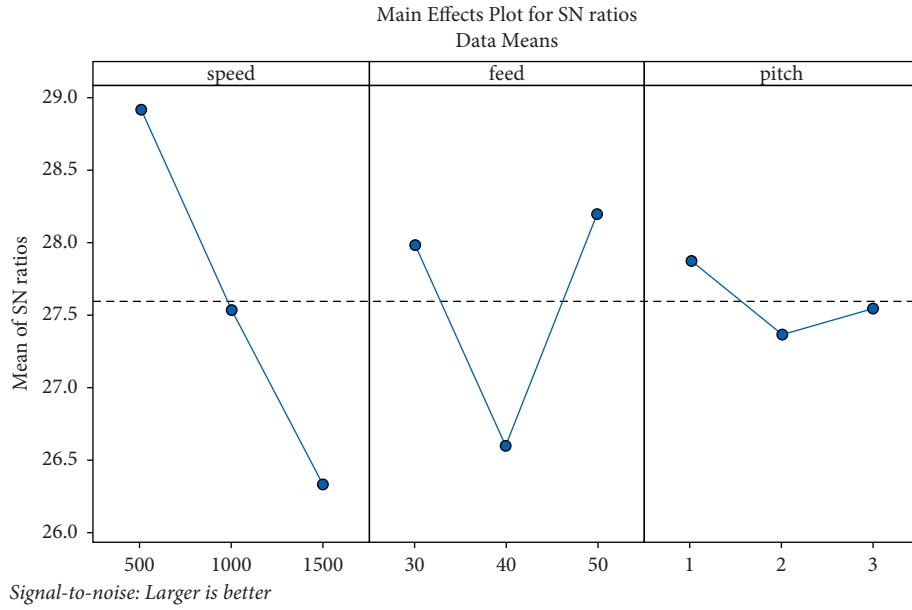


FIGURE 6: Main effect plot for S/N ratio of UTS.

TABLE 7: Response for S/N ratios of hardness.

Level	TRS	Feed rate	Pitch
1	37.61	38.45	38.59
2	38.81	38.30	38.38
3	39.12	38.80	38.57
Delta	1.51	0.51	0.21
Rank	1	2	3

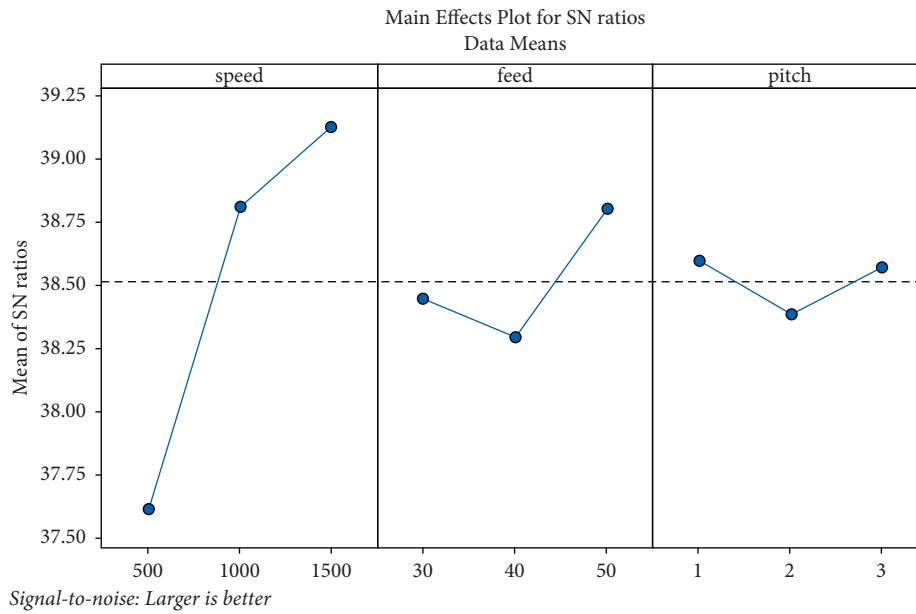


FIGURE 7: Main effect plot for S/N ratio of hardness.

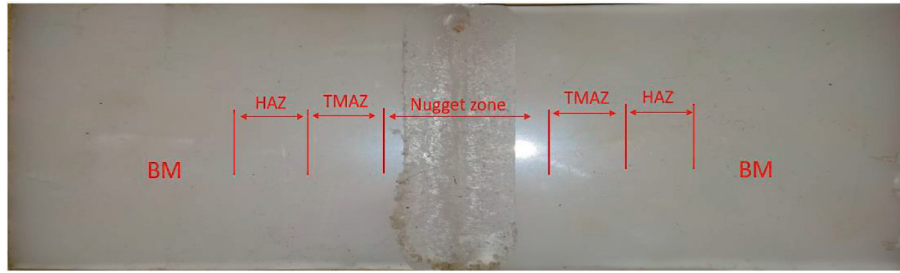


FIGURE 8: Formed zones in the weld cutaway in the FSW method.

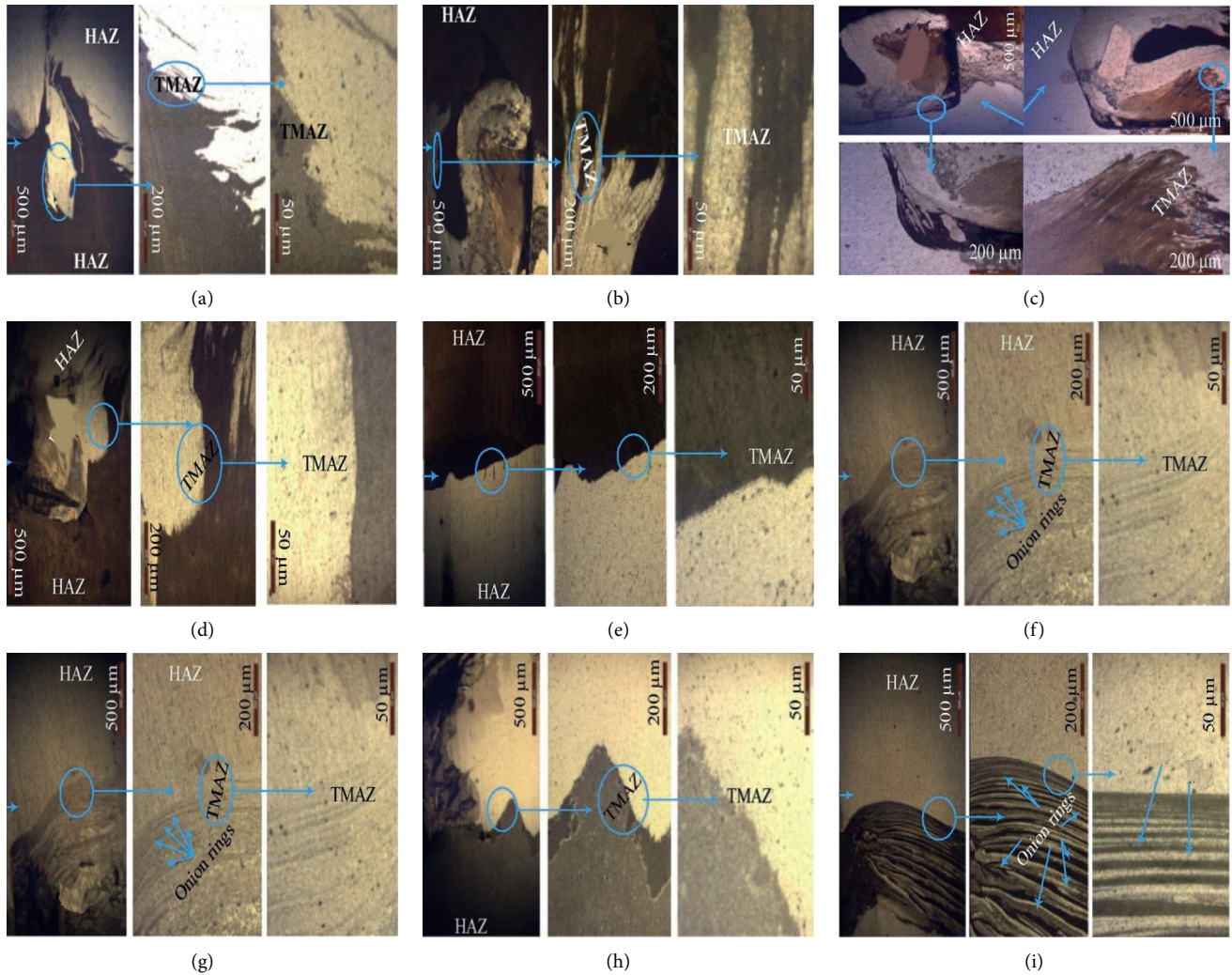


FIGURE 9: Obtained microstructural images with different welding parameters. (a) TRS: 500 rpm, and feed rate: 30 mm/min. (b) TRS: 500 rpm, and feed rate: 40 mm/min. (c) TRS: 500 rpm, and feed rate: 50 mm/min. (d) TRS: 1000 rpm, and feed rate: 30 mm/min. (e) TRS: 1000 rpm, and feed rate: 40 mm/min. (f) TRS: 1000 rpm, and feed rate: 50 mm/min. (g) TRS: 1500 rpm, and feed rate: 30 mm/min. (h) TRS: 1500 rpm, and feed rate: 40 mm/min. (i) TRS: 1500 rpm, and feed rate: 50 mm/min.

5. Conclusion

This article proposed an experimental investigation of FSW process on nylon 6A polymer material using the HCHCr

tool with taper threaded tool profile by varying the pitch values. In addition, optimal process parameters are obtained using Taguchi's L_{27} orthogonal array approach. Further, ANOVA with regression equations is also done to disclose

the effectiveness of input operating process parameters impact on the output responses like UTS and hardness. The final conclusions made from the obtained experimental and optimized results are as follows:

- (i) The results of Taguchi proved that the mathematical models have an ability to forecast the parameters of FSW with the confidence interval of 95%
- (ii) The most significant and the least significant FSW parameters are the tool rotation and feed rate, respectively
- (iii) The parameters like feed and TRS were considered for FSW joints UTS of nylon 6A polymer composite
- (iv) The optimum FSW parameters such as the feed rate of 30 mm/min, tool pitch of 3 mm, and the TRS of 500 rpm obtained the maximum UTS

The FSW technique joined with the micro- and macrostructures of welding joints has shown that the varied welding seams relied on welding parameters, which has impacted the value of hardness. The major difference between hardness values of joints was the differing hardness values with the heat influence although the joints' hardness values were made with both pin geometries. In the experiments, the lowest and highest hardness values have been computed. The maximum and minimum hardness values were obtained for the feed rate of 30 mm/min, TRS of 1500 rpm and the feed rate of 50 mm/min, TRS of 500 rpm, respectively.

Data Availability

The data used to support the findings of this study are included within the article.

Disclosure

This study was performed as a part of the Employment of Addis Ababa Science and Technology University, Addis Ababa, Ethiopia.

Conflicts of Interest

The authors declare that there are no conflicts of interest regarding this study.

References

- [1] S. R. Strand, *Effects of Friction Stir Welding on Polymer Microstructure*, Theses and Dissertations, Brigham Young University, Provo, Utah, 2004.
- [2] M. Barmouz, P. Shahi, and P. Asadi, "Friction stir welding/processing of polymeric materials," *Advances in Friction-Stir Welding and Processing*, Elsevier, Amsterdam, Netherlands, pp. 601–670, 2014.
- [3] A. Pramanik, A. K. Basak, Y. Dong et al., "Joining of carbon fibre reinforced polymer (CFRP) composites and aluminium alloys - a review," *Composites Part A: Applied Science and Manufacturing*, vol. 101, pp. 1–29, 2017.
- [4] A. Mostafapour and F. Taghizad Asad, "Investigations on joining of Nylon 6 plates via novel method of heat assisted friction stir welding to find the optimum process parameters," *Science and Technology of Welding & Joining*, vol. 21, no. 8, pp. 660–669, 2016.
- [5] R. S. Mishra and Z. Y. Ma, "Friction stir welding and processing," *Materials Science and Engineering: R: Reports*, vol. 50, no. 1–2, pp. 1–78, 2005.
- [6] S. Eslami, P. J. Tavares, and P. M. G. P. Moreira, "Friction stir welding tooling for polymers: review and prospects," *International Journal of Advanced Manufacturing Technology*, vol. 89, no. 5–8, pp. 1677–1690, 2017.
- [7] T. W. Nelson, C. D. Sorenson, and C. J. Johns, "Friction stir welding of polymeric materials," US Patent, US01014501, 2001.
- [8] J. Gao, X. Cui, C. Liu, and Y. Shen, "Application and exploration of friction stir welding/processing in plastics industry," *Materials Science and Technology*, vol. 33, no. 10, pp. 1145–1158, 2017.
- [9] H. Ahmadi, N. B. Mostafa Arab, and F. A. Ghasemi, "Optimization of process parameters for friction stir lap welding of carbon fiber reinforced thermoplastic composites by Taguchi method," *Journal of Mechanical Science and Technology*, vol. 28, pp. 278–284, 2014.
- [10] G. H. Payganeh, N. B. Mostafa Arab, Y. Dadgar Asl, F. A. Ghasemi, and M. Saeidi Boroujeni, "Effects of friction stir welding process parameters on appearance and strength of polypropylene composite welds," *International Journal of the Physical Sciences*, vol. 6, no. 19, pp. 4595–4601, 2011.
- [11] Z. Kiss and T. Czigány, "Effect of welding parameters on the heat affected zone and the mechanical properties of friction stir welded poly(ethylene-terephthalate-glycol)," *Journal of Applied Polymer Science*, vol. 125, no. 3, pp. 2231–2238, 2012.
- [12] A. Zafar, M. Awang, S. R. Khan, and S. Emamian, "Investigating friction stir welding on thick Nylon 6 plates," *Welding Journal*, vol. 95, no. 6, pp. 210–218, 2016.
- [13] F. Simões and D. M. Rodrigues, "Material flow and thermo-mechanical conditions during friction stir welding of polymers: literature review, experimental results and empirical analysis," *Materials & Design*, vol. 59, pp. 344–351, 2014.
- [14] N. Sadeghian and M. K. Besharati Givi, "Experimental optimization of the mechanical properties of friction stir welded Acrylonitrile Butadiene Styrene sheets," *Materials & Design*, vol. 67, pp. 145–153, 2015.
- [15] F. Lambiase, A. Paoletti, and A. Di Ilio, "Effect of tool geometry on mechanical behavior of friction stir spot welds of polycarbonate sheets," *International Journal of Advanced Manufacturing Technology*, vol. 88, no. 9–12, pp. 3005–3016, 2016.
- [16] B. Kusharjanta, W. Raharjo, and Triyono, "Temperature comparison of initial, middle and final point of polypropylene friction stir welded," *AIP Conference Proceedings*, vol. 1717, Article ID 040011, 2016.
- [17] S. Saeedy and M. K. B. Givi, "Investigation of the effects of critical process parameters of friction stir welding of polyethylene," *Proceedings of the Institution of Mechanical Engineers - Part B: Journal of Engineering Manufacture*, vol. 225, no. 8, pp. 1305–1310, 2011.
- [18] K. Raza, M. Shamir, M. K. A. Qureshi, A. S. Shaikh, and M. Zain-ul-abdein, "On the friction stir welding, tool design optimization, and strain rate-dependent mechanical properties of HDPE-ceramic composite joints," *Journal of Thermoplastic Composite Materials*, vol. 31, no. 3, pp. 291–310, 2018.
- [19] V. K. S. Jain, J. Varghese, and S. Muthukumaran, "Effect of first and second passes on microstructure and wear properties

- of titanium dioxide-reinforced aluminum surface composite via friction stir processing,” *Arabian Journal for Science and Engineering*, vol. 44, no. 2, pp. 949–957, 2019.
- [20] Y. Huang, X. Meng, Y. Xie et al., “Friction stir welding/processing of polymers and polymer matrix composites,” *Composites Part A: Applied Science and Manufacturing*, vol. 105, pp. 235–257, 2018.
- [21] H. Laieghi, S. Alipour, and A. Mostafapour, “Heat-assisted friction stir welding of polymeric nanocomposite,” *Science and Technology of Welding & Joining*, vol. 25, no. 1, pp. 56–65, 2020.
- [22] X. Meng, Y. Huang, Y. Xie et al., “Friction self-riveting welding between polymer matrix composites and metals,” *Composites Part A: Applied Science and Manufacturing*, vol. 127, Article ID 105624, 2019.
- [23] I. Khan, G. Hussain, K. A. Al-Ghamdi, and R. Umer, “Investigation of impact strength and hardness of UHMW polyethylene composites reinforced with nano-hydroxyapatite particles fabricated by friction stir processing,” *Polymers*, vol. 11, no. 6, p. 1041, 2019.
- [24] W. Ratanathavorn, “Hybrid joining of aluminum to thermoplastics with friction stir welding,” Dissertation, 2012.
- [25] M. G. Bidgolia, A. Ranjbaran, K. Mirzavand, Y. Shajari, Z. Seyedraoufi, and M. Porhonor, “Investigation of carbon fiber reinforced polymer composite welding with a new tool in friction stir welding method,” *International Journal of Engineering Transactions C: Aspects*, vol. 32, no. 6, pp. 860–865, 2019.
- [26] S. P. Meyer, B. Jaeger, C. Wunderling, and M. F. Zaeh, “Friction stir welding of glass fiber-reinforced polyamide 6: analysis of the tensile strength and fiber length distribution of friction stir welded PA6-GF30,” *IOP Conference Series: Materials Science and Engineering*, vol. 480, Article ID 012013, 2019.
- [27] M. R. Hajideh, O. Shapurgan, N. M. Ramzani, and E. H. Nejad, “Friction stir welding of dissimilar poly methyl methacrylate and polycarbonate sheets,” *Journal of Modern Processes in Manufacturing and Production*, vol. 6, no. 4, 2017.
- [28] A. Zafar, M. Awang, S. R. Khan, and S. Emamian, “Role of pin profile on material flow during friction stir welding of nylon 6,” *ARPJ Journal of Engineering*, vol. 11, no. 22, 2016.
- [29] S. Kumar, T. Medhi, and B. S. Roy, “Friction stir welding of thermoplastic composites,” in *Advances in Industrial and Production Engineering*, K. Shanker, R. Shankar, and R. Sindhvani, Eds., Springer, SingaporeSpringer, 2019 Lecture Notes in Mechanical Engineering.
- [30] H. Kumar and S. V. Satish, “Friction stir welding of polymeric materials,” *International Journal of Engineering Research and Technology*, vol. 9, no. 6, pp. 697–699, 2020.